Localization of Rayleigh waves

B. Garber and M. Cahay
Department of Electrical and Computer Engineering and Computer Science, University of Cincinnati, Cincinnati, Ohio 45221

G. E. W. Bauer
Faculty of Applied Physics, Delft University of Technology, Lorentzweg 1, 2628 CJ Delft, The Netherlands
(Received 30 March 2000)

We study the localization of Rayleigh waves propagating in a semi-infinite and isotropic medium with inhomogeneities that are modeled as rods parallel to the incoming wave front and are distributed randomly up to a maximum depth. For a perfectly smooth surface, the localization length of a Rayleigh wave is predicted to reach a minimum at intermediate wavelength λ and to diverge for both low and large values of λ. For large λ, the divergence results from the fact that the strength of each scatterer is proportional to ω^2, where ω is the angular frequency of the incident Rayleigh wave. For small λ, the divergence results from Rayleigh waves propagating closer to the surface and therefore being sensitive to a decreasing number of impurities.

I. INTRODUCTION

Multiple scattering is a phenomenon generic to wave propagation in inhomogeneous media which can lead to an exponential attenuation of a wave, even in the absence of any dissipative mechanism. This phenomenon is usually referred to as localization and was predicted in 1958 by Anderson for electrons propagating in disordered solids.[1] Since then, it has now been well established both theoretically and experimentally that, even with an infinitesimal amount of randomness, all waves (Schrödinger and classical) are localized in systems with spatial dimensions less than or equal to two.[2]

For acoustic (seismic) waves, a thorough understanding of practically relevant effects, such as disorder-induced delocalization transition in randomly stratified media, wave conversion between seismic shear and pressure waves, and geological information in the coda of seismic shot records, should improve the quantitative analysis of seismograms of the interior of the earth. Up to now, there has been only a few investigations of the possibility of localization of acoustic and seismic waves.[3]

The frequency dependence of the localization length Λ_{loc} for acoustic waves in one-dimensional randomly layered media has been studied both numerically and analytically by Sheng and co-workers.[4,5] They showed that beyond the low-frequency behavior of $\Lambda_{\mathrm{loc}} \sim \omega^{-2}$, where ω denotes the angular frequency, the localization length either approaches a constant or diverges at high frequencies. In all cases the values of Λ_{loc} for a given random medium was found to exhibit a well-defined lower bound value generally several orders of magnitude times the correlation length between impurities. White and co-workers used Sheng's localization theory to successfully interpret the backscattering spectra of seismic waves recorded in sonic well logs from diverse geological environments.[6]

Recently, Meseguer *et al.* have studied the scattering of Rayleigh waves by a periodic array of cylindrical holes drilled perpendicular to the surface of a marble quarry.[7] The cylindrical holes were arranged in periodic arrays of both honeycomb and triangular lattices. By recording the attenuation spectra of the surface waves, Meseguer *et al.* observed the existence of absolute band gaps for elastic waves in these semi-infinite two-dimensional crystals. As a possible application of their investigations, they suggested the controlled attenuation of surface waves generated by earthquakes.

In this paper we focus on the propagation of surface waves (Rayleigh waves) and determine their localization length as a function of frequency in the presence of impurities (scatterers) close to the surface. The characterization of Rayleigh waves propagating in disordered media is important for several reasons. Rayleigh waves are often quite damaging in the propagation of earthquakes and also produce a ground-roll noise in the interpretation of seismic records.[8] Surface wave studies have also received increased attention from civil engineers over the last 15 years for imaging the subsurface using the so-called SASW technique (spectral analysis of surface waves).[9–11] Some applications of the SASW method include the detection of buried stream channels in rocks, the determination of the depth of trenches filled with debris from a bombing range, and the detection and delineation of buried cavities, among others.[12]

Hereafter, we consider the simple problem of Rayleigh propagation through a half-space occupied by an isotropic homogeneous linearly elastic material in the presence of a random array of inhomogeneities. The analysis presented here is not readily applicable to the interpretation of Rayleigh wave propagation through stratified media which are more representative of the actual earth crust,[9] but it can serve as a benchmark calculation in the development of more sophisticated models.

This paper is organized as follows. In Sec. II we describe the scattering-matrix formalism used to determine the wavelength dependence of the localization length for Rayleigh waves normally incident on a two-dimensional array of circular rods parallel to the surface of a semi-infinite medium. Section III describes the results of numerical simulations. Section IV contains our conclusions.

II. APPROACH

In 1970 Steg and Klemens used the Born approximation to study the scattering of Rayleigh waves by surface irregu-

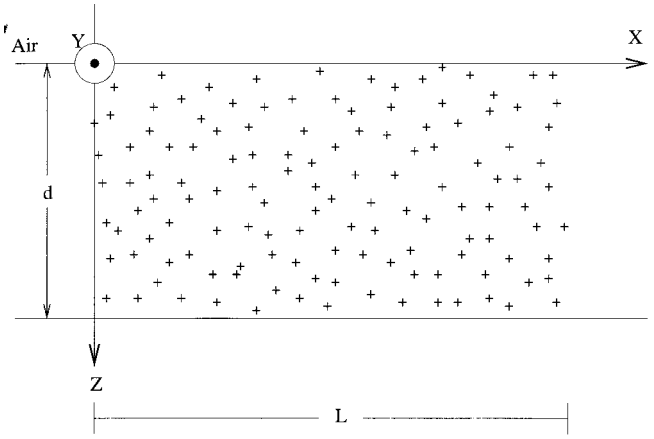

FIG. 1. Illustration of a one-dimensional array of circular rods distributed randomly up to a finite depth in a semi-infinite homogeneous and isotropic medium. The rods are parallel to the *y* axis and the Rayleigh waves are incident from left to right and propagate along the *x* direction. The circular rods are modeled as two-dimensional δ scatterers.

larities (mass defects) as a function of frequency and defect depth.[13] They argued that the most general solution to this problem requires two kinds of scattered waves, namely Rayleigh waves of different propagation directions and body waves (longitudinal and transverse). Steg and Klemens have shown that when impurities are less than a wavelength below the surface, the Rayleigh waves scatter almost exclusively into other Rayleigh waves of the same frequency but different directions. Using a first-order Born approximation for surface irregularities, the scattering rate of the primary Rayleigh wave was found to vary as the fifth power of frequency. In the present paper we consider scattering centers below the surface which we model as lines parallel to the incoming wave front so that the problem is kept two-dimensional for simplicity. Hereafter, we neglect the mixing between surface waves and body waves. The scattering rate of Rayleigh waves into other Rayleigh waves is one order of magnitude larger than the scattering rate into body waves as long as $kd<3$,[13] where k is the wave number of the incoming Rayleigh wave and d is the depth of the impurity. A more thorough analysis, including the effects of bulk waves, would tend to decrease the transmission of Rayleigh waves along the surface, eventually leading to a shorter localization length than predicted in this paper. Finally, we assume that the cross section of the two-dimensional impurities are small compared to the wavelength of the surface waves and we model them as δ scatterers. The geometry of the problem is illustrated in Fig. 1.

We consider a Rayleigh wave with a fixed frequency incident from the left on a two-dimensional disordered array of scatterers located in a region of length L along the x axis. The scatterers are assumed to be parallel to the y axis and randomly distributed up to a maximum depth d.

Experimentally, a study of the localization of Rayleigh waves would require the placement of geophones on the surface or deep inside the semi-infinite half space in order to record the power per unit area delivered by the surface wave.[14] For a geophone with its membrane placed perpendicular to the propagation of the surface wave (x direction in Fig. 1), the power per unit area will be proportional to the square of the transmission amplitude through the array $|T|^2$. Hereafter, we describe a scattering-matrix technique to determine the transmission coefficient of the Rayleigh wave as a function of frequency of the primary surface wave. If localization occurs as a result of the multiple interference of waves through the disordered array, we expect $|T|^2$ to be of the form

$$|T|^2 \sim \exp(-L/\Lambda_{\mathrm{loc}}), \tag{1}$$

where Λ_{loc} is the localization length. Numerically, the inverse of the localization length is then determined using the following procedure

$$1/\Lambda_{\mathrm{loc}} = -1/L\langle \ln|T|^2\rangle \tag{2}$$

as L goes to infinity, where the brackets denote configurational averaging.

Since the rods have a small cross section, Navier's equation for the spatial variation of the medium displacement becomes[14]

$$\begin{bmatrix} (\lambda+2\mu)\dfrac{d^2}{dx^2}+\mu\dfrac{d^2}{dz^2} & (\lambda+\mu)\dfrac{d^2}{dxdz} \\ (\lambda+\mu)\dfrac{d^2}{dxdz} & (\lambda+2\mu)\dfrac{d^2}{dz^2}+\mu\dfrac{d^2}{dx^2} \end{bmatrix} \begin{bmatrix} u(x,z) \\ w(x,z) \end{bmatrix} + \omega^2 \left[\rho_0 + \sum_i \rho_i \delta(x-x_i)\delta(z-z_i) \right] \begin{bmatrix} u(x,z) \\ w(x,z) \end{bmatrix} = \begin{bmatrix} 0 \\ 0 \end{bmatrix}, \tag{3}$$

where ρ_0 is the density of the background (semi-infinite medium), ρ_i is a parameter characterizing the strength of the δ scatterers located at (x_i, z_i). It is assumed to be the same for all impurities and its magnitude will be determined below. The $(u(x,z), w(x,z))$ are the components of the medium displacement along the x and z axis, respectively. The (λ,μ) parameters are the Lamé constants of the background medium.[15] These parameters are related to the bulk phase velocity of primary (V_p) and secondary waves (V_s) through the relations $\mu=\rho_0 V_s^2$ and $\lambda+2\mu=\rho_0 V_p^2$.[15] Hereafter, we have neglected the difference between the Lamé parameters of the rods and background material for simplicity.

At any point (x,z), the solution of the equation above describing Rayleigh wave propagation along the surface is given by Ref. 15

$$\begin{bmatrix} u(x,z) \\ w(x,z) \end{bmatrix} = \begin{bmatrix} f_1(z) \\ f_2(z) \end{bmatrix} g_k(x), \tag{4}$$

where the functions f_1, f_2 are given explicitly in the Appendix. In the absence of scatterers, the function $g_k(x)$ is a simple plane wave with wave number $k=\omega/C_R$, where C_R and ω are the phase velocity and angular frequency of the incident Rayleigh wave, respectively. For a semi-infinite, homogeneous and isotropic medium, it is well known that Rayleigh waves are dispersionless, i.e., C_R is independent of frequency.[15] In the neighborhood of the surface, for a Rayleigh wave propagating from left to right in Fig. 1, the medium motion is elliptical and counterclockwise in the xz plane, with a vertical displacement about 1.5 times the horizontal displacement. The horizontal motion is reduced to

zero at a depth of about 0.2 times the Rayleigh wavelength. The medium becomes elliptical and clockwise at greater depth.

In the presence of disorder, the function $g_k(x)$ between two adjacent impurities along the x axis is a superposition of left- and right-going plane waves

$$g_k(x)=A_+e^{-jkx}+A_-e^{+jkx}. \tag{5}$$

If we consider a Rayleigh wave incident from the left, we have

$$g_k(x)=e^{-jkx}+Re^{+jkx} \tag{6}$$

for $x<0$, and

$$g_k(x)=Te^{-jkx} \tag{7}$$

for $x>L$.

To find $g_k(x)$ anywhere in region $[0,L]$, we first derive a differential equation for g_k starting with Eq. (3). Substituting Eq. (4) in Eq. (3), multiplying on the left by row vector (f_1^*,f_2^*) (where the asterisk stands for complex conjugate), and integrating from $z=0$ to ∞, we obtain

$$[(\lambda+2\mu)\alpha_1+\mu\alpha_2]\ddot{g}_k(x)+(\lambda+\mu)(\beta_1+\beta_2)\dot{g}_k(x)+[(\lambda+2\mu)\gamma_2+\mu\gamma_1]g_k(x)+\omega^2\left(\rho_0(\alpha_1+\alpha_2)+\sum_i \rho_i\eta_i\delta(x-x_i)\right)g_k(x)=0, \tag{8}$$

where the dot stands for d/dx. In Eq. (8), some short-hand notations have been used by introducing the coefficients (α_1,α_2), (β_1,β_2), and (γ_1,γ_2), written explicitly in the Appendix. Furthermore, the coefficients η_i are defined as follows:

$$\eta_i=f_1^*(z_i)f_1(z_i)+f_2^*(z_i)f_2(z_i). \tag{9}$$

At the location x_i of the ith rod, we require $g_k(x)$ to be continuous. Furthermore, starting with Eq. (8) and integrating across the ith scatterer, i.e., over the interval $]x_i-\epsilon,x_i+\epsilon[$ and letting ϵ go to zero, we get

$$[(\lambda+2\mu)\alpha_1+\mu\alpha_2][\dot{g}_k(x_i^+)-\dot{g}_k(x_i^-)]+\omega^2\sum_i \eta_i\rho_i g_k(x_i)=0. \tag{10}$$

To calculate the overall transmission coefficient across the entire array, we use a scattering-matrix approach with the cascading rules given, for instance, in Ref. 16. This requires the derivation of the scattering-matrix across an individual scatterer (S_i)

$$S_i=\begin{bmatrix} T_i & R_i' \\ R_i & T_i' \end{bmatrix}, \tag{11}$$

where the (R_i,T_i) are the reflection and transmission amplitudes across the scatterer for a Rayleigh wave incident from the left and (R_i',T_i') are the reflection and transmission amplitudes for a wave incident from the right. To determine (R_i,T_i) (which is independent of the location of the scatterer along the x axis), we consider the scattering problem across a single δ scatterer at location $(0,z_i)$. Continuity of $g_k(x)$ at $x=0$ implies

$$1+R_i=T_i, \tag{12}$$

whereas Eq. (10) leads to

$$[(\lambda+2\mu)\alpha_1+\mu\alpha_2][-jkT_i+jk-jkR_i]+\omega^2\rho_iR_i\eta_iT_i=0. \tag{13}$$

This last equation can be rewritten as follows:

$$\epsilon_iT_i-jk\tilde{\alpha}R_i=-jk\tilde{\alpha}, \tag{14}$$

where

$$\epsilon_i=\omega^2\rho_iR_i\eta_i-jk\tilde{\alpha} \tag{15}$$

and

$$\tilde{\alpha}=(\lambda+2\mu)\alpha_1+\mu\alpha_2. \tag{16}$$

Multiplying Eq. (12) on both sides by ϵ_i, we get

$$\epsilon_iT_i-\epsilon_iR_i=\epsilon_i, \tag{17}$$

which can be solved simultaneously with Eq. (14) to find R_i and T_i. We obtain

$$R_i=\frac{\omega^2\rho_i\eta_i}{[2jk\tilde{\alpha}-\omega^2\rho_i\eta_i]}, \tag{18}$$

and

$$T_i=\frac{2jk\tilde{\alpha}}{[2jk\tilde{\alpha}-\omega^2\rho_i\eta_i]}. \tag{19}$$

It can be easily shown that

$$|R_i|^2+|T_i|^2=1. \tag{20}$$

Furthermore, because of the symmetry of the problem we have

$$R_i'=R_i \tag{21}$$

and

$$T_i'=T_i. \tag{22}$$

For the array of scatterers, the overall scattering-matrix entire array can then be obtained by cascading scattering matrices for δ scatterers with the scattering matrices representing the phase shifts between scatterers.[16]

Before we proceed with numerical examples, we first analyze in more detail the properties of the transmission coefficient through a single scatterer. Referring back to Eq. (19), T_i is seen to depend on the parameters α_1, α_2, and η_i. Starting with the definitions given in the Appendix, we find

$$\alpha_1=|\phi_0|^2\left[\frac{1}{2\kappa_p}k^2+\frac{1}{2}\delta^2\kappa_s-2k\delta\left(\frac{\kappa_s}{\kappa_s+\kappa_p}\right)\right] \tag{23}$$

and

$$\alpha_2=|\phi_0|^2\left[\frac{\kappa_p}{2}+\frac{1}{2}k^2\left(\frac{\delta^2}{\kappa_s}\right)-2k\delta\left(\frac{\kappa_p}{\kappa_s+\kappa_p}\right)\right], \tag{24}$$

where

$$\kappa_p=Ak \tag{25}$$

and

$$\kappa_s = Bk, \tag{26}$$

where $A=\sqrt{1-(C_R/V_p)^2}$ and $B=\sqrt{1-(C_R/V_s)^2}$. In Eqs. (23) and (24), $\delta=\sqrt{A/B}$ is the ratio between the normal and tangential particle displacement of the Rayleigh wave propagating on the free surface of the semi-infinite medium.[17] Furthermore, ϕ_0 is the maximum amplitude of the Rayleigh wave in the x direction. Since α_1, α_2, and η_i are all proportional to $|\phi_0|^2$, the coefficients R_i, T_i are independent of ϕ_0. Setting $\phi_0=1$ in Eqs. (23) and (24) and using the definitions of the parameters κ_s, κ_p, we get

$$\alpha_{1,2} = C_{1,2}k, \tag{27}$$

where the parameters C_1 and C_2 are independent of frequency and are given by

$$C_1 = 1/2A + \delta^2/2B - 2\delta A/(A+B) \tag{28}$$

and

$$C_2 = A/2 + \delta^2/2B - 2\delta A/(A+B). \tag{29}$$

Furthermore, using the definitions (A1) and (A2) in the Appendix and setting $\phi_0=1$, we obtain

$$\eta_i = k^2 f(kR) \tag{30}$$

where

$$\begin{aligned} f(kR) = {} & (1+A^2)e^{-2(kR)A(z_i/R)} \\ & + (1+B^2)\delta^2 e^{-2(kR)B(z_i/R)} \\ & - 2\delta(A+B)e^{-(kR)(B+A)(z_i/R)}. \end{aligned} \tag{31}$$

Using the results above, the transmission amplitude T_i becomes simply

$$T_i = \frac{jb}{jb-a} \tag{32}$$

with

$$a = k^4 \rho_i C_R^2 f(kR) \tag{33}$$

and

$$b = 2k^2[(\lambda+2\mu)C_1 + \mu C_2]. \tag{34}$$

For a typical impurity, the strength of the scatterer ρ_i (with dimensions $\mathrm{Kg\,m^{-1}}$) is determined by imposing the following condition:

$$\int\int dx\,dz\,\rho_i \delta(x-x_i)\,\delta(z-z_i) = \pi R^2(\rho_r - \rho_0) = \pi R^2 \Delta\rho, \tag{35}$$

where R is the radius of the circular rod, ρ_r the density of the rod material, and we have assumed that $z_i > R$. The right-hand side of Eq. (35) ensures that ρ_i is equal to zero when ρ_r is equal to ρ_0, as it should in the absence of a scatterer.

Using Eqs. (32)–(35) we can rewrite the transmission amplitude as

$$T_i = \frac{2j[C_1(V_p^2/V_s^2)+C_2]}{2j[C_1(V_p^2/V_s^2)+C_2] - \pi(\Delta\rho/\rho_0)(C_R/V_s)^2(kR)^2 f(kR)}. \tag{36}$$

The frequency dependence of the transmission coefficient $|T_i|^2$ is therefore controled by the frequency dependence of the term $(kR)^4 f^2(kR)$.

One-dimensional (1D) limit. If the scatterers are all at the same depth z_i, the problem is purely one-dimensional and the localization length is equal to the elastic mean free path.[3] Using reduced units in which the localization length is expressed as the average number of impurities crossed,[16] the localization length can be calculated as follows:

$$\Lambda_{\mathrm{loc}} = |T_i|^2/|R_i|^2 = |b|^2/|a|^2. \tag{37}$$

The actual localization length must then be obtained by multiplying this number by the average distance between impurities in the x direction.

The qualitative dependence of the localization length as a function of the Rayleigh-wave wavelength can be estimated as follows. From Eqs. (36) and (37), we obtain

$$\Lambda_{\mathrm{loc}} \sim \lambda^4 / f^2(\lambda). \tag{38}$$

For $\lambda\to\infty$, $f^2(\lambda)$ reduces to a constant and $\Lambda_{\mathrm{loc}}\sim\lambda^4$. For $\lambda\to 0$ (i.e., $\omega\to\infty$) and since $B-A<0$, we have

$$f(kR) \sim e^{-2kRB(z_i/R)}(1+B^2)\delta^2, \tag{39}$$

leading to

$$\lambda_{\mathrm{loc}} \sim \lambda^4 e^{\lambda_0/\lambda}, \tag{40}$$

where

$$\lambda_0 = 8\pi B z_i. \tag{41}$$

Therefore, we expect the localization length (or elastic mean free path) to reach a minimum at a wavelength λ^* given by

$$\lambda^* \sim \lambda_0/4. \tag{42}$$

If the z_i's are random (with $R<z_i$ for our model to be valid), we still expect the localization length to diverge for both small and large wavelengths and therefore to reach a minimum for some specific λ^*. Indeed, for small frequency, the transmission amplitude across any scatterer is close to unity (independent of their location) since their scattering strength is proportional to ω^2. Because we use a δ-scatterer model for the impurities, the theory is valid for values of λ down to $\sim 2R$, or equivalently for kR values up to $\sim\pi$ (see the numerical examples below). For small λ and fixed z_i, the function $f(kR)$ exponentially goes down to zero. This corresponds to the fact that Rayleigh waves of high frequency are

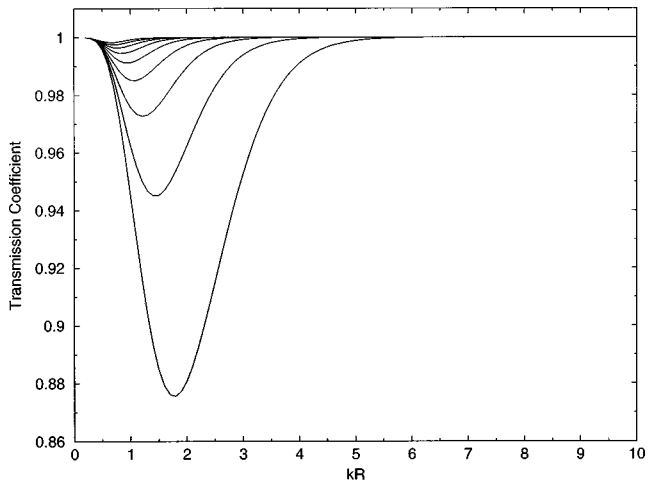

FIG. 2. Plot of the transmission coefficient through a single impurity as a function of the parameters kR for different values of $z_R = z_i/R$, where k is the wave number of the Rayleigh wave, R is the radius of the circular rod, and z_i is the depth of the ith impurity. From bottom to top, the curves correspond to z_R varying from 2 to 6, in steps of 0.5.

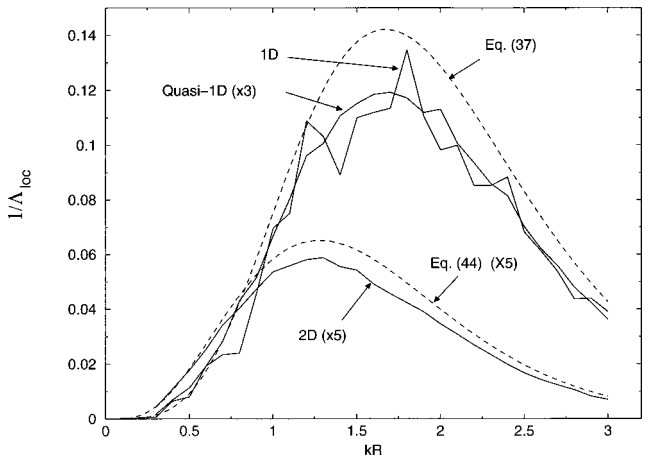

FIG. 3. Plot of the inverse of the localization length versus the parameter $kR = \omega R/C_R$. The full lines are the inverse of the localization length calculated using Eq. (2) while averaging over 1000 samples. The dashed line is the result derived using Eq. (37). The localization length is in units of the number of impurities crossed in the x direction. The simulations are for different disordered arrays of impurities. The curve labeled 1D corresponds to impurities all at the same depth $z_i = 2R$ but distributed randomly along the x axis ($x_i = [8i + 3.99\ \mathrm{ran}(i)]R$, where ran($i$) is a uniform random number between $[-1,+1]$). The curve labeled ''Quasi-1D'' corresponds to samples made of three 1D arrays located at depths equal to $2R$, $5R$, and $8R$, respectively. The curve labeled 2D corresponds to the two-dimensional disordered samples described in the text.

propagating closer to the surface, a phenomenon quite analogous to the skin effect for high-frequency current moving through metals. As a result, for $\lambda \to 0$, the impurities located below the surface do not affect Rayleigh-wave propagation. Even for the impurities close to the surface, the transmission coefficient eventually approaches unity as the frequency increases. In other words, there are fewer and fewer scatterers felt by the Rayleigh waves as the frequency approaches infinity and the localization therefore diverges as $\lambda^{-1} \to \infty$. The prediction of a minimum of the localization length at an intermediate value of kR is therefore expected to hold even for more advanced models for the scatterers. Only the location of the minimum along the kR axis is expected to change.

In the next section we describe simulation results for the frequency dependence of the localization length of Rayleigh waves calculated using Eq. (2).

III. RESULTS

Hereafter, we consider arrays of two-dimensional elastic scatterers distributed along the x and z axes. The z_i locations are assumed to be less than or equal to a maximum depth d. We only take into account disorder due to the random locations of the rods and assume all ρ_i's in Eq. (3) to be identical. The strength ρ_i of each scatterer is fixed using Eq. (35). In the simulations, the density of the semi-infinite medium and rods is set equal to 7.8×10^3 and 15.5×10^3 Kg/m^3, respectively.[18] For the background medium, the primary (V_p) and secondary (V_s) wave velocities are selected to be 5800 and 3100 m/s, respectively.[14] In that case, the phase velocity of Rayleigh waves along the x axis is calculated to be 2876 m/s, a value independent of frequency for a semi-infinite medium.[15]

Figure 2 is a plot of the transmission coefficient across a single impurity versus kR for different values of z_i/R. We note the following features: first, for a fixed z_i/R, the transmission coefficient is close to unity for both low and large values of kR. This is in agreement with the fact that, for low kR, Rayleigh waves extend over a region much larger than the impurity size. The impurity acts as a weak scatterer and the transmission coefficient through the impurity is close to unity. Second, for sufficiently large kR, Rayleigh waves are located closer to the free surface and decay over a length scale shorter than the location z_i of the fixed impurity, hence the transmission coefficient is also close to unity. This last assertion is true independent of the model of the scatterer.

Case 1: 1D random arrays. We first consider disordered arrays of scatterers with the location of the ith impurity selected as follows $(x(i),z(i)) = ([8i + 3.99\ \mathrm{ran}(i)]R, 2R)$, where R is the radius of the circular rod and ran(i) is a uniform random number between -1 and $+1$. Since all impurities have the same depth, this case corresponds to the 1D limit analysis in Sec. II. The full line in Fig. 3 is a plot of the inverse localization length calculated using Eq. (2) while averaging over 1000 samples. The analytical expression for the inverse localization length [Eq. (37)] is plotted as a function of the parameter kR and is a very good fit to the numerical results. The localization length reaches a minimum for $\lambda^* \sim \lambda_0/4$ where λ_0 is given by Eq. (41). For the 1D array considered here $8\pi B \sim 7.5$, $z_i = 2R$, and therefore $\lambda^* \sim 3.75R$. As a result, we expect $1/\Lambda_{\mathrm{loc}}$ to reach a maximum for a value of kR equal to $2\pi R/\lambda^* \sim 1.7$. This value is in good agreement with the numerical results shown in Fig. 3 and is below 2, the value above which the δ-scatterer model breaks down.

According to the analysis of Steg and Klemens,[13] the scattering rate of Rayleigh waves into bulk waves is negligible as long as $kd < 3$. In our case, the depth of each impurity is equal to $2R$. Therefore, past $kR = 1.5$, we expect the trans-

mission coefficient through the array, and therefore the effective localization length, to decrease below the value predicted here. This may lead to a shift and larger value of the maximum shown in Fig. 3. However, at high frequencies, the coupling to the bulk waves is suppressed and we still expect the localization length to diverge in this limit. The maximum observed in Fig. 3 is therefore expected to be at least qualitatively correct. With the inclusion of bulk waves, the range of kR values at which we expect the minimum localization length can be estimated as follows. The amplitude of Rayleigh waves in the z direction is related to the magnitude of the functions (f_1, f_2) in Eq. (4). From the expressions given in the Appendix, both f_1 and f_2 become negligible at the depth z_i of the impurity array whenever, say,

$$kBz_i \sim 5. \tag{43}$$

Since $z_i = 2R$ and $8\pi B \sim 7.5$, the amplitude of the incident Rayleigh wave at z_i is negligible whenever $kR \sim 8$. No bulk waves can be generated by the impurities at depth z_i past that limit. The effects of surface roughness could become important, however, past $kR \sim 8$, as discussed below. As a numerical example, if we select $R = 1$ mm, the theory above predicts that the minimum localization length of the system considered above would reach a value of 6.7 cm for a Rayleigh wave excited on the surface at a frequency of 0.78 MHz.

Next, we consider arrays of impurities composed of three layers of 1D arrays of scatterers with their x locations selected as in the previous example and with their depth equal to $2R$, $5R$, and $8R$, respectively. For the impurities at depth equal to $5R$ and $8R$, the transmission coefficient is near unity, as can be seen in Fig. 2. The impurities at these depths merely introduce an additional phase shift between the impurities located at the top array. Expressed as an average number of impurities crossed, the localization length is therefore expected to be three times longer than in the previous example. Expressed in meters, the localization length is, however, the same as in the previous example since the density of impurities per unit length along the x axis is three times larger than in the 1D case considered above. This last numerical simulation shows that the wavelength dependence of the localization length of Rayleigh waves is merely affected by scatterers close to the surface.

Case 2: Two-dimensional (2D) random arrays. In this last example, we calculate the localization length of 2D disordered samples generated as follows. The depth of each impurity is selected randomly and uniformly between $2R$ and $8R$. We generate block of five impurities at a time with their x location selected randomly in each block j with a uniform distribution over the interval $[8(j-1), 8j]R$. This generation of impurities block by block is made in order to avoid the time-consuming sorting process of the x location of the impurities if they are generated randomly over the entire length of the sample. In Fig. 3 we plot the average (over 1000 samples) of the inverse of the localization length. Again, we observe a nonmonotonous behavior of the localization length with a minimum at a value different from the one predicted for a purely 1D array of scatterers. This is because the transmission coefficient for the impurities close to the surface have different magnitudes when the depth of the impurities is allowed to vary. The main feature of this last example is that the occurrence of the minimum in the localization length of Rayleigh waves is still observed for 2D arrays.

Actually, for the case of 2D arrays of impurities, the inverse of the localization length can be estimated starting with Eq. (37) and calculating the weighted average

$$1/\Lambda_{\mathrm{loc}} = 1/6R \int_{2R}^{8R} dz_i |R_i|^2/|T_i|^2, \tag{44}$$

where R_i and T_i are given by Eqs. (18) and (19), respectively. A plot of this average value is shown as a dashed line in Fig. 3. Stated otherwise, the 2D arrays of scatterers can be interpreted as 1D arrays of scatterers with a scattering strength obtained using the averaging procedure above.

IV. CONCLUSIONS

We have used a scattering-matrix approach to study the localization length of Rayleigh waves propagating in a semi-infinite medium in the presence of a random array of one-dimensional circular rods with a density different from the density of the semi-infinite medium. For simplicity, the wave front of the incident waves was assumed to be perpendicular to the two-dimensional δ scatterers. The latter are parallel to the surface of the semi-infinite medium and are located up to a maximum depth.

The localization length is found to diverge at both large and small values of the wavelength of the incident Rayleigh wave and to reach a minimum at an intermediate wavelength. This behavior is expected independent of the model of the scatterer. At low wavelength, the divergence is expected since the strength of the scatterers vanishes as ω^2. At large frequencies, Rayleigh waves are located closer to the surface and are therefore sensitive to a smaller number of scatterers.

In our analysis, the assumption of 1D scatterers parallel to the y axis in Fig. 1 was made for simplicity. For scatterers whose extent along the y axis would be shorter than the wavelength, the analysis would need to be repeated with fully 3D scatterers. These scatterers would induce diffuse scattering, i.e., coupling between Rayleigh waves with different (k_x, k_z) wave-vector components. This would increase the localization length at any particular wavelength. However, the localization length would still be expected to diverge at large and small values of the wavelength because the arguments given above hold also for 3D scatterers. Therefore, even for this more general case, the localization length is a nonmonotonic function of the wavelength and reaches a minimum at some intermediate λ.

ACKNOWLEDGMENTS

The authors would like to thank P. Nagy and A. Nayfeh for their helpful comments throughout this work. This research was supported by the Technology Foundation STW, applied science division of NWO and the technology program of the Dutch Ministry of Economic Affairs. B.G. and M.C. acknowledge the hospitality of the Applied Physics Department at Delft University of Technology where part of this work was accomplished.

APPENDIX

The functions f_1 and f_2 defined in Eq. (4) and describing the propagation of Rayleigh waves through a semi-infinite medium can be calculated explicitly,[15]

$$f_1(z)=jk\left\{-\exp\left[-k\sqrt{1-\left(\frac{C_R}{V_p}\right)^2}z\right]+\delta\sqrt{1-\left(\frac{C_R}{V_s}\right)^2}\times\exp\left[-k\sqrt{1-\left(\frac{C_R}{V_s}\right)^2}z\right]\right\} \tag{A1}$$

and

$$f_2(z)=k\left\{-\sqrt{1-\left(\frac{C_R}{V_p}\right)^2}\exp\left[-k\sqrt{1-\left(\frac{C_R}{V_p}\right)^2}z\right]+\delta\exp\left[-k\sqrt{1-\left(\frac{C_R}{V_s}\right)^2}z\right]\right\}, \tag{A2}$$

where δ is given by

$$\delta=\frac{2-(C_R/V_s)^2}{2\sqrt{1-(C_R/V_s)^2}} \tag{A3}$$

and $k=\omega/C_R$ is the wave number, C_R and ω being the phase velocity and angular frequency of the incident Rayleigh wave, respectively. The coefficients (α_1,α_2), (β_1,β_2), and (γ_1,γ_2) in Eq. (8) are defined as follows:

$$\alpha_1=\int_0^{+\infty}dz f_1^*(z)f_1(z), \tag{A4}$$

$$\alpha_2=\int_0^{+\infty}dz f_2^*(z)f_2(z), \tag{A5}$$

$$\beta_1=\int_0^{+\infty}dz f_1^*(z)\frac{df_2(z)}{dz}, \tag{A6}$$

$$\beta_2=\int_0^{+\infty}dz f_2^*(z)\frac{df_1(z)}{dz}, \tag{A7}$$

$$\gamma_1=\int_0^{+\infty}dz f_1^*(z)\frac{d^2f_1(z)}{dz^2}, \tag{A8}$$

and

$$\gamma_2=\int_0^{+\infty}dz f_2^*(z)\frac{d^2f_2(z)}{dz^2}. \tag{A9}$$

[1] P. W. Anderson, Phys. Rev. **109**, 1492 (1958).

[2] P. A. Lee and T. V. Ramakrishnan, Rev. Mod. Phys. **57**, 287 (1985).

[3] P. Sheng, *Introduction to Wave Scattering, Localization, and Mesocopic Phenomena* (Academic, New York, 1995).

[4] P. Sheng, Z.-Q. Zhang, B. White, and G. Papanicolaou, Phys. Rev. Lett. **57**, 1000 (1986).

[5] P. Sheng, B. White, Z.-Q. Zhang, and G. Papanicolaou, Phys. Rev. B **34**, 4757 (1986).

[6] B. White, P. Sheng, and B. Nair, Geophysics **55**, 1158 (1990).

[7] F. Meseguer, M. Holgado, D. Cabarello, N. Benaches, J. Sanchez-Dehesa, C. Lopez, and J. Llinares, Phys. Rev. B **59**, 12 169 (1999).

[8] K. Aki and P. L. Richards, *Quantitative Seismology, Theory and Methods* (Freeman, San Francisco, 1980).

[9] K. H. Stokoe II, S. G. Wright, J. A. Bay, and J. M. Roesset, *Geophysical Characterization of Sites*, edited by R. D. Woods (Oxford and IBH, New Delhi, 1994), pp. 15–25.

[10] M. Dravinski, Earthquake Eng. Struct. Dyn. **11**, 313 (1993).

[11] N. Gucunski, V. Ganji, and M. Maher, Soil Dyn. Earthquake Eng. **15**, 223 (1996).

[12] B. A. Luke, C. T. Begley, D. S. Chase, A. J. Ross, and J. E. Brady, *Proceedings of 10th Annual Symposium on the Application of Geophysics to Engineering and Environmental Problems* (Environmental and Engineering Geophysical Society, Reno, Nevada, 1997), pp. 983–992.

[13] R. G. Steg and P. G. Klemens, Phys. Rev. Lett. **24**, 381 (1970).

[14] L. W. Schmerr, Jr., *Fundamental of Ultrasonic Nondestructive Evaluation, A Modeling Approach* (Plenum, New York, 1998), p. 119.

[15] M. Lavergne, *Seismic Methods* (Graham and Trotman Ltd., Sterling House, London, 1989).

[16] M. Cahay, M. McLennan, and S. Datta, Phys. Rev. B **37**, 10 125 (1988).

[17] W. Hassan and P. B. Nagy, J. Acoust. Soc. Am. **104**, 3107 (1998).

[18] This system would correspond to a background medium made out of stainless steel containing rods made of some type of alloy with a mixture of gold, tungsten, or platinum and some lighter metal.